Volume Integral Equations for Analysis of Dielectric Branching Waveguides

KAZUO TANAKA, MEMBER, IEEE, AND MASAAKI KOJIMA

Abstract—New forms of volume integral equations are developed for the exact treatment of wave propagation in two-dimensional dielectric branching waveguides. The new integral equations can be obtained by considering the condition at a point far away from the junction section. An approximate solution by the Born approximation and a numberical solution by the moment method established the validity of the new volume integral equations. The numerical results are discussed from the viewpoint of energy conservation and reciprocity. The solution is exact if sufficiently large computer memory and computational time are employed.

I. Introduction

The DIELECTRIC branching waveguide is a basic element in integrated circuits operating in the range from millimeter to optical wavelengths. It is important to know the basic characteristics of electromagnetic wave propagation in the branching waveguide. It is not easy, however, to analyze the wave propagation in detail in these complex waveguide configurations. A variety of techniques have been developed to make the problem mathematically tractable. The beam propagation method (BPM), first introduced by Feit and Fleck [1], is often used to calculate transmission characteristics and radiation losses in the branching waveguide [2]–[6]. Seino *et al.* analyzed the intersecting waveguide by the improved BPM [7]. Approximate step theory, first developed by Marcuse [8], is also used to calculate mode conversion in branching waveguides [9]–[12]. Kuznetsov and Haus [13] and Kuznetsov [14] used the volume current method (VCM), which was originally formulated by Snyder [15], to calculate the radiation loss from several complex waveguide configurations. Common shortcomings of all these analyses are their approximate treatment of the problem, and the accuracy of the results obtained by these approximate techniques has not been checked by techniques based on an exact treatment.

In order to treat wave propagation in the dielectric branching waveguides exactly, new forms of volume integral equations (VIE) are presented in this paper [16]. This was advanced for use in the numerical analysis of scattering problems by dielectric objects of general shapes [17], [18] and the technique is related to the VCM. We regard the problem of wave propagation in the dielectric branching waveguide as a scattering problem. Since the waveguide has infinite size, the original form of VIE cannot be applied directly to the problem containing dielectric waveguides of infinite length such as branching waveguides.

The new VIE's which are applicable to the branching waveguide are derived by introducing specific conditions at points far away from the waveguide junction, and these VIE's can be solved by conventional methods. This is illustrated using the Born approximation and the moment method. The validity of the new VIE's is discussed from the viewpoint of energy conservation and reciprocity. Since the treatment of the problem is exact, the numerical solution becomes very accurate if sufficiently large computer memory and computational times are employed.

II. Geometry of the Problem

The dielectric branching waveguide geometry considered in this paper is shown in Fig. 1. We confine our attention to two-dimensional dielectric waveguides due to their mathematical simplicity. The time factor $\exp(j\omega t)$ is understood. In this paper, we treat grounded branching waveguide due to the mathematical simplicity of the Green's function. The branching waveguide, which has no grounded plane, can be treated similarly by introducing a proper Green's function. Waveguide 1 plus waveguide 2 constitute one straight dielectric waveguide of normalized thickness k_0a located on a perfectly conducting plane at $y=-a$ in Fig. 1, where $k_0=\omega/c$ and c is the velocity of light in free space. Waveguide 3, of normalized thickness $2k_0b$, is connected directly to the straight waveguide with junction angle ϕ, as shown in Fig. 1. It is assumed that indices of refraction of dielectric waveguides 1, 2, and 3 are given by n_1, n_1, and n_2, respectively, surrounded by free space. It is also assumed that all waveguides satisfy the single-mode condition and that the propagating mode is a TE mode only.

Since the electric fields have only a z component under the above-mentioned conditions, we can denote electric field intensity in the coordinate systems (x, y), (X, Y), and (r, θ) in Fig. 1 as

$$E_z(\vec{x})=E(x,y)=E(X,Y)=E(r,\theta). \qquad (1)$$

First consider the case where the TE-odd dominant mode is incident from waveguide 1 to the junction section as shown in Fig. 1. The incident wave is expressed in the $x-y$

Manuscript received June 29, 1987; revised March 15, 1988.
K. Tanaka is with the Department of Electronics and Computer Engineering, Gifu University, Yanagido 1-1, 501-11 Japan.
M. Kojima was with the Department of Electronics and Computer Engineering, Gifu University, Yanagido 1-1, 501-11, Japan. He is now with the Nippon Telegraph and Telephone Corporation, Tokyo, Japan.
IEEE Log Number 8821760.

0018-9480/88/0800-1239$01.00

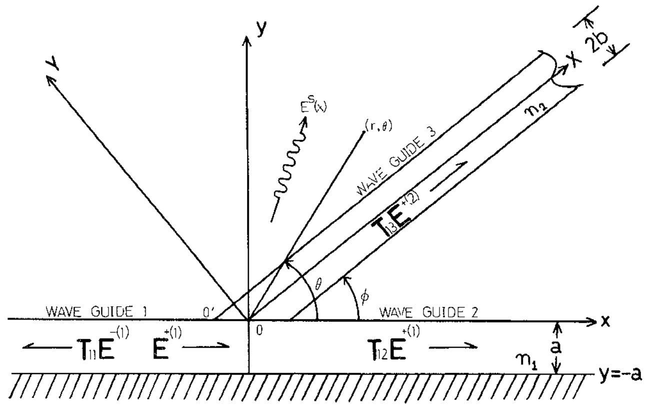

Fig. 1. Geometry of the problem.

coordinates of Fig. 1 by

$$E^{+(1)}(\vec{x}) = f(y)\exp(-j\beta_1 x) \tag{2}$$

where

$$f(y) = \begin{cases} \sin[\kappa_1(y+a)] & (-a \leqslant y \leqslant 0) \\ \sin(\kappa_1 a)\exp(-\delta_1 y) & (0 < y) \end{cases} \tag{3}$$

and

$$\kappa_1 = (n_1^2 k_0^2 - \beta_1^2)^{1/2} \qquad \delta_1 = (\beta_1^2 - k_0^2)^{1/2}. \tag{4}$$

The reflected wave in waveguide 1, the transmitted wave in waveguide 2, and the transmitted wave in waveguide 3 can be expressed as

$$T_{11}E^{-(1)}(\vec{x}) = T_{11}f(y)\exp(+j\beta_1 x)$$
$$T_{12}E^{+(1)}(\vec{x}) = T_{12}f(y)\exp(-j\beta_1 x)$$
$$T_{13}E^{+(2)}(\vec{x}) = T_{13}F(Y)\exp(-j\beta_2 X) \tag{5}$$

respectively, where a constant T_{ij} $(i, j = 1,2,3)$ means the transmission coefficient in the jth waveguide for the case of incidence from the ith waveguide. Therefore, T_{11} and T_{12} are the reflection and transmission coefficient in waveguides 1 and 2, respectively, and T_{13} is the transmission coefficient in waveguide 3. Function $F(Y)$ in the $X-Y$ coordinates of Fig. 1 can be expressed as

$$F(Y) = \begin{cases} \cos(\kappa_2 Y), & |Y| \leqslant b \\ \cos(\kappa_2 b)\exp[\delta_2(b-Y)], & Y > b \\ \cos(\kappa_2 b)\exp[\delta_2(b+Y)], & Y < -b \end{cases} \tag{6}$$

where

$$\kappa_2 = (n_2^2 k_0^2 - \beta_2^2)^{1/2} \qquad \delta_2 = (\beta_2^2 - k_0^2)^{1/2} \tag{7}$$

and the propagation constants β_1 and β_2 are determined by the dispersion relations given by

$$\kappa_1\cos(\kappa_1 a) + \delta_1\sin(\kappa_1 a) = 0 \qquad \text{(in waveguides 1 and 2)}$$
$$\kappa_2\sin(\kappa_2 b) - \delta_2\cos(\kappa_2 b) = 0 \qquad \text{(in waveguide 3)}. \tag{8}$$

III. Integral Equations

From Maxwell's equations and Green's theorem, the well-known volume integral equation for the total electric field $E(\vec{x})$ is [17]

$$E(\vec{x}) = k_0^2 \iint_{\text{semi-infinite space } x' > 0} [n^2(\vec{x}') - 1] G(\vec{x}|\vec{x}') \cdot E(\vec{x}')\, d\vec{x}' + E^{+(1)}(\vec{x})$$
$$= k_0^2(n_2^2 - 1)\iint_S G(\vec{x}|\vec{x}')E(\vec{x}')\, d\vec{x}' + E^{+(1)}(\vec{x}) \tag{9}$$

where $n(\vec{x})$ represents the distribution of the index of refraction of the medium, with $n(\vec{x}) = n_2$ in waveguide 3, and $n(\vec{x}) = 1$ in the surrounding space. In (9), $G(\vec{x}|\vec{x}')$ is the Green's function of the system, where only waveguide 1 plus 2 exists on the metal plane. Therefore, the surface integral in (9) extends over the infinite domain S of the dielectric waveguide 3.

The total electric fields in waveguide 3 created by the incident wave are very complicated. Only the transmitted surface wave can survive at points far away from the junction in waveguide 3. Hence, we assume that the total electric fields in waveguide 3 can be decomposed into two components as

$$E(\vec{x}) = E^C(\vec{x}) + T_{13}E^{+(2)}(\vec{x}). \tag{10}$$

In (10), $E^C(\vec{x})$ means the electric field given by subtraction of the transmitted surface wave from the total fields created by the branching discontinuity in the direction of wave propagation in waveguide 3. We call $E^C(\vec{x})$ the disturbed field. It can be seen that the disturbed field is confined to the vicinity of the junction section; i.e., it will satisfy the following condition:

$$E^C(\vec{x}) = 0 \qquad (\theta = \phi, r \to \infty). \tag{11}$$

Substituting (10) into (9), we consider the condition which must hold at a point far away from the junction section in waveguide 3. If the distance $k_0 r$ from the origin O in Fig. 1 is sufficiently large, condition (11) shows that the following relation must hold:

$$T_{13}E^{+(2)}(\vec{x}) = k_0^2(n_2^2-1)\iint_S G(r,\phi|\vec{x}')E^C(\vec{x}')\, d\vec{x}' + T_{13}k_0^2(n_2^2-1)\iint_S G(r,\phi|\vec{x}')E^{+(2)}(\vec{x}')\, d\vec{x}' \qquad (r \to \infty). \tag{12}$$

Therefore, the transmission coefficient T_{13} can be expressed as

$$T_{13} = \frac{k_0^2(n_2^2-1)\iint_S G(r,\phi|\vec{x}')E^C(\vec{x}')\, d\vec{x}'}{E^{+(2)}(r,\phi) - k_0^2(n_2^2-1)\iint_S G(r,\phi|\vec{x}')E^{+(2)}(\vec{x}')\, d\vec{x}'} \qquad (r \to \infty). \tag{13}$$

Using Green's theorem, we can reduce the surface integral in the denominator of (13) into a line integral as follows:

$$E^{+(2)}(\vec{x}) - k_0^2(n_2^2-1)\iint_S G(r,\phi|\vec{x}')E^{+(2)}(\vec{x}')\,d\vec{x}' = -\int_C \left[E^{+(2)}(\vec{x}')\frac{\partial G(r,\phi|\vec{x}')}{\partial n'} - \frac{\partial E^{+(2)}(\vec{x}')}{\partial n'} \cdot G(r,\phi|\vec{x}')\right] dl' \quad (14)$$

where $\partial/\partial n' = -\partial/\partial y'$ and contour C corresponds to the line $y=0$ in Fig. 1. Since $k_0 r$ is a large value in (14), we can expand the Green's function in terms of $1/(k_0 r)$ by using saddle-point integration [19] as

$$G(r,\theta|\vec{x}') = A(r)g(\theta|\vec{x}') + O\left[(k_0 r)^{-3/2}\right] \quad (15)$$

where

$$A(r) = -j/4[2/(\pi k_0 r)]^{1/2}\cdot\exp(-jk_0 r + j\pi/4). \quad (16)$$

We first substitute (14) into (13), substitute expression (15) into the resultant expression, and then divide the numerator and denominator by the common function $A(r)$. Putting $k_0 r \to \infty$, the transmission coefficient T_{13} can be expressed in terms of the disturbed field $E^C(\vec{x})$ as

$$T_{13} = k_0^2(n_2^2-1)\iint_S g(\phi|\vec{x}')E^C(\vec{x}')\,d\vec{x}'/M_{+2}(\phi) \quad (17)$$

where the constant $M_{+2}(\phi)$ is given by

$$M_{+2}(\phi) = M_{+2}(\theta)|_{\theta=\phi} = -\int_C \left[E^{+(2)}(\vec{x}')\frac{\partial g(\theta|\vec{x}')}{\partial n'} - \frac{\partial E^{+(2)}(\vec{x}')}{\partial n'} \cdot g(\theta|\vec{x}')\right] dl' \Big|_{\theta=\phi} \quad (18)$$

and this line integral can be readily evaluated. Substituting (17) and (10) into (9) and using Green's theorem again, we finally obtain the new form of the VIE for the disturbed field $E^C(\vec{x})$ as follows:

$$E^C(\vec{x}) = k_0^2(n_2^2-1)\iint_S P(\vec{x}|\vec{x}')E^C(\vec{x}')\,d\vec{x}' + E^{+(1)}(\vec{x}) \quad (19)$$

where

$$P(\vec{x}|\vec{x}') = G(\vec{x}|\vec{x}') + g(\phi|\vec{x}')S_{+2}(\vec{x})/M_{+2}(\phi) \quad (20)$$

and

$$S_{+2}(\vec{x}) = \int_C \left[E^{+(2)}(\vec{x}')\frac{\partial G(\vec{x}|\vec{x}')}{\partial n'} - \frac{\partial E^{+(2)}(\vec{x}')}{\partial n'}G(\vec{x}|\vec{x}')\right] dl'. \quad (21)$$

As in (9), the two-dimensional integral in VIE (19) extends over the infinite domain of dielectric waveguide 3. However, the disturbed field $E^C(\vec{x})$ becomes zero sufficiently far away from the junction point. Hence we can consider that the infinite domain S in (19) is reduced to the finite domain, where $E^C(\vec{x})$ is assumed not to be zero.

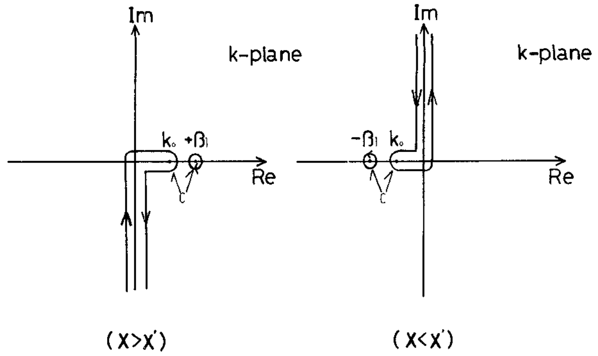

Fig. 2. Illustration of contour c in the Fourier integral (22).

IV. The Green's Function

The Green's function $G(\vec{x}|\vec{x}')$ in (9) is the solution of the problems of an electric current line source located at $\vec{x}=\vec{x}'$ above waveguides 1 plus 2. The result can be written as a Fourier transform [19]:

$$G(\vec{x}|\vec{x}') = \frac{1}{4\pi}\int_c \left\{\frac{1}{jp}\exp(-jp|y-y'|) - \frac{1}{jp} \cdot R(k)\exp[-jp(y+y')]\right\}\exp[-jk(x-x')]\,dk \quad (22)$$

where

$$R(k) = [q\cos(qa) - jp\sin(qa)] / [q\cos(qa) + jp\sin(qa)]$$
$$p = (k_0^2 - k^2)^{1/2} \qquad q = (n_1^2 k_0^2 - k^2)^{1/2}. \quad (23)$$

A contour c in (22) is illustrated in Fig. 2. The branch-cut integrals represent the radiation fields, and residues at the enclosed poles are the surface-wave modes in waveguides 1 and 2. The function $g(\theta|\vec{x}')$ can be obtained through saddle-point integration as

$$g(\theta|\vec{x}') = \exp(jk_0 x'\cos\theta + jk_0 y'\sin\theta) - R(k_0\cos\theta)\exp(jk_0 x'\cos\theta - jk_0 y'\sin\theta). \quad (24)$$

V. Reflected Wave, Transmitted Wave, and Scattered Waves

Once the disturbed field $E^C(\vec{x})$ has been determined, the transmission coefficient T_{12} in waveguide 2, the reflection coefficient T_{11} in waveguide 1, and the scattered waves in the surrounding space can be expressed by the disturbed field. Substituting (10) into the original integral equation (9), we calculate residues of Green's function (22). By using (14), the transmission and reflection coefficients can be expressed as

$$T_{11} = -j/2A_s k_0^2(n_2^2-1)\iint_S \exp(-\delta_1 y' - j\beta_1 x') \cdot E^C(\vec{x}')\,d\vec{x}' + j/2T_{13}A_s \cdot \int_C\left[-\delta_1 E^{+(2)}(\vec{x}')\exp(-j\beta_1 x') + \frac{\partial E^{+(2)}(\vec{x}')}{\partial n'}\exp(-j\beta_1 x')\right]dl' \tag{25}$$

$$T_{12} = -j/2A_s k_0^2(n_2^2-1) \cdot \iint_S \exp(-\delta_1 y' + j\beta_1 x')E^C(\vec{x}')\,d\vec{x}' + j/2T_{13}A_s\int_C\left[-\delta_1 E^{+(2)}(\vec{x}')\exp(j\beta_1 x') + \frac{\partial E^{+(2)}(\vec{x}')}{\partial n'}\exp(j\beta_1 x')\right]dl' + \sin(\kappa_1 a) \tag{26}$$

respectively, where

$$A_s = 2(n_2^2k_0^2 - \beta_1^2)/\{k_0^2(n_2^2-1)[\beta_1/\delta_1 + \beta_1 a]\}. \tag{27}$$

The scattered waves $E^S(r,\theta)$ can be obtained in similar fashion by using the saddle-point integration of Green's function as

$$E^S(r,\theta) = A(r)B_1(\theta) \tag{28}$$

where

$$B_1(\theta) = k_0^2(n_2^2-1)\iint_S g(\theta|\vec{x}')E^C(\vec{x}')\,d\vec{x}' - T_{13}M_{+2}(\theta). \tag{29}$$

We notice from (17) and (29) that the scattered wave (28) becomes zero at junction angle $\theta = \phi$. The reflected, transmitted, and scattered powers normalized to the incident wave power can be obtained by calculating the time-averaged Poynting vector, and they are given by

$$\Gamma_{11} = |T_{11}|^2/\sin(\kappa_1 a) \tag{30}$$

$$\Gamma_{12} = |T_{12}|^2/\sin(\kappa_1 a) \tag{31}$$

$$\Gamma_{13} = 2|T_{13}|^2 U/W \tag{32}$$

$$\Gamma_{1S} = 1/(8\pi)\cdot\int_0^\pi |B_1(\theta)|^2\,d\theta/W \tag{33}$$

respectively, where Γ_{iS} $(i=1,2,3)$ represents scattered power normalized to the incident wave power for the case of incidence from the ith waveguide and the constants U and W are given by

$$U = \beta_2[b/2 + 1/(4\kappa_2)\sin(2\kappa_2 b) + 1/(2\delta_2)\cos^2(\kappa_2 b)] \tag{34}$$

$$W = \beta_1[a/2 - 1/(4\kappa_1)\sin(2\kappa_1 a) + 1/(2\delta_1)\sin^2(\kappa_1 a)]. \tag{35}$$

For the case where the TE-odd dominant mode is incident from waveguide 2, all the results can be obtained in the same way as in the case of incidence from waveguide 1.

VI. Incidence From Waveguide 3

We next consider the case where the TE-even dominant mode is incident from waveguide 3. We substitute the total field expression

$$E(\vec{x}) = E^C(\vec{x}) + T_{33}E^{+(2)}(\vec{x}) + E^{-(2)}(\vec{x}) \tag{36}$$

into (9), where $E^{+(1)}(\vec{x})$ is omitted. In (36), $E^{-(2)}(\vec{x})$ represents the incident wave given by

$$E^{-(2)}(\vec{x}) = F(Y)\exp(j\beta_2 X). \tag{37}$$

Using relations (14) and (15) and Green's theorem, the resultant VIE is found to be

$$E^C(\vec{x}) = k_0^2(n_2^2-1)\iint_S P(\vec{x}|\vec{x}')E^C(\vec{x}')\,d\vec{x}' + M_{-2}(\phi)/M_{+2}(\phi)S_{+2}(\vec{x}) + S_{-2}(\vec{x}) \tag{38}$$

where

$$S_{-2}(\vec{x}) = \int_C\left[E^{-(2)}(\vec{x}')\frac{\partial G(\vec{x}|\vec{x}')}{\partial n'} - \frac{\partial E^{-(2)}(\vec{x}')}{\partial n'}G(\vec{x}|\vec{x}')\right]dl' \tag{39}$$

and where the constant $M_{-2}(\phi)$ is given by

$$M_{-2}(\phi) = M_{-2}(\theta)\Big|_{\theta=\phi} = -\int_C\left[E^{-(2)}(\vec{x}')\frac{\partial g(\theta|\vec{x}')}{\partial n'} - \frac{\partial E^{-(2)}(\vec{x}')}{\partial n'}g(\theta|\vec{x}')\right]dl'\Bigg|_{\theta=\phi}. \tag{40}$$

If the disturbed field $E^C(\vec{x})$ is obtained, the transmission coefficients T_{31} and T_{32} is waveguides 1 and 2, the reflection coefficient T_{33} in waveguide 3, and the scattered waves in the surrounding space can be expressed as

$$T_{31} = -j/2A_s k_0^2(n_2^2-1) \cdot \iint_S \exp(-\delta_1 y' - j\beta_1 x')E^C(\vec{x}')\,d\vec{x}' + j/2T_{33}A_S\int_C\left[-\delta_1 E^{+(2)}(\vec{x}')\exp(-j\beta_1 x') + \frac{\partial E^{+(2)}(\vec{x}')}{\partial n'}\exp(-j\beta_1 x')\right]dl' + j/2A_S\int_C\left[-\delta_1 E^{-(2)}(\vec{x}')\exp(-j\beta_1 x') + \frac{\partial E^{-(2)}(\vec{x}')}{\partial n'}\exp(-j\beta_1 x')\right]dl' \tag{41}$$

$$T_{32} = -j/2A_S k_0^2(n_2^2-1) \cdot \iint_S \exp(-\delta_1 y' + j\beta_1 x') E^C(\vec{x}')\, d\vec{x}' + j/2T_{33}A_S \int_C \left[-\delta_1 E^{+(2)}(\vec{x}') \exp(j\beta_1 x') + \frac{\partial E^{+(2)}(\vec{x}')}{\partial n'} \exp(j\beta_1 x') \right] dl' + j/2A_S \int_C \left[-\delta_1 E^{-(2)}(\vec{x}') \exp(j\beta_1 x') + \frac{\partial E^{-(2)}(\vec{x}')}{\partial n'} \exp(j\beta_1 x') \right] dl' \quad (42)$$

$$T_{33} = \left[k_0^2(n_2^2-1) \iint_S g(\phi|\vec{x}') E^C(\vec{x}')\, d\vec{x}' - M_{-2}(\phi) \right] / M_{+2}(\phi) \quad (43)$$

$$B_3(\theta) = k_0^2(n_2^2-1) \iint_S g(\theta|\vec{x}') E^C(\vec{x}')\, d\vec{x}' - T_{33} M_{+2}(\theta) - M_{-2}(\theta). \quad (44)$$

VII. Energy Conservation and Reciprocity

The total power must satisfy the energy conservation law, and this relation can be written as

$$\sum_{j=1}^{3} \Gamma_{ij} + \Gamma_{iS} = \Gamma_{\mathrm{TOTAL}} = 1 \qquad (i=1,2,3). \quad (45)$$

This relation can be used to check the numerical results. The transmission coefficient or reflection coefficient T_{ij} $(i, j=1,2,3)$ must satisfy the reciprocity condition (symmetric property of the scattering matrix) and this relation can be written as

$$\Gamma_{ij} = \Gamma_{ji} \qquad (i, j=1,2,3). \quad (46)$$

This relation also can be used to check the results.

VIII. The Born Approximation

The new forms of VIE's, (19) and (38), can be solved by various techniques. Two techniques are used in this paper, i.e., the Born approximation and the moment method. The most simple approximate solution can be obtained by replacing the disturbed field $E^C(\vec{x})$ by known functions. The most simple case is by using information for the incident waves. We call this approximation the Born approximation and put

$$E^C(\vec{x}) = E^{\pm(1)}(\vec{x}) \qquad \begin{array}{l} + : \text{incident from waveguide 1} \\ - : \text{incident from waveguide 2} \end{array} \quad (47)$$

$$E^C(\vec{x}) = 0 \qquad \text{(incident from waveguide 3)}. \quad (48)$$

Substituting expressions (47) and (48) into the expressions for T_{ij}, all the reflection and transmission coefficients can be evaluated easily and can be expressed analytically. The actual expressions are omitted in this paper.

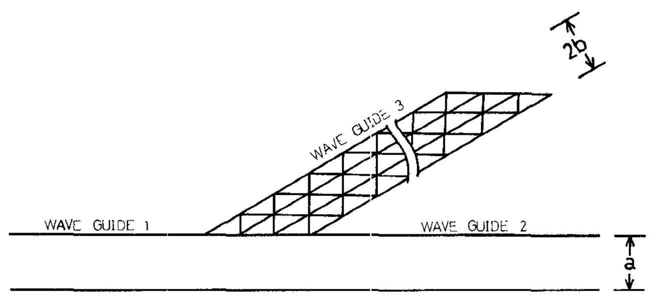

Fig. 3. Division of waveguide 3 into right triangles.

IX. Moment Method

We solve integral equations (19) and (38) numerically by the moment method by dividing the domain of waveguide 3 into many right triangular elements, as shown in Fig. 3, which are small enough so that the disturbed electric field intensity in each element is expressed by linear functions given by

$$E_i^C(x, y) = A_i x + B_i y + C_i. \quad (49)$$

In (49), A_i, B_i, and C_i are linear functions of values $E^C(\vec{x})$ at vertices of the triangle, where the subscript i refers to a particular element i. The disturbed electric field intensity at each vertex is initially considered to be an unknown quantity. Substituting (49) into (19) or (38) and performing the line and surface integrals on the right-hand side of (19) or (38), we enforce the VIE (19) or (38) at each vertex. When we perform the line and surface integrals in (19) and (38), we first perform the integral with respect to variables x' and y' analytically, and then perform the Fourier integral with respect to variable k numerically along the contour c illustrated in Fig. 2. A system of N linear equations can be obtained finally, where N is the total number of vertices. The system of linear equations can be solved numerically and numerical values at each vertex obtained. If a sufficiently large number of triangles with sufficiently small area is used, the solution will approach the exact solution.

X. Numerical Examples

In the numerical calculations using the moment method, we divide waveguide 3 into 642 triangles which have 432 vertices. For the case of $\phi = 30°$, $k_0 a = 2.0$, $2k_0 b = 1.0$, and $n_1 = n_2 = 1.5$, the numerical results of the disturbed fields $E^C(x)$ along the upper side of waveguide 3 are shown in Figs. 4–6 for the case of incidence from waveguide 1, 2, and 3, respectively. In Figs. 4–6, the abscissa represents the normalized distance from the junction point O' in Fig. 1 and the solid and dotted lines show the real and imaginary parts of $E^C(\vec{x})$, respectively. We see that the disturbed field $E^C(\vec{x})$ becomes negligible far from the

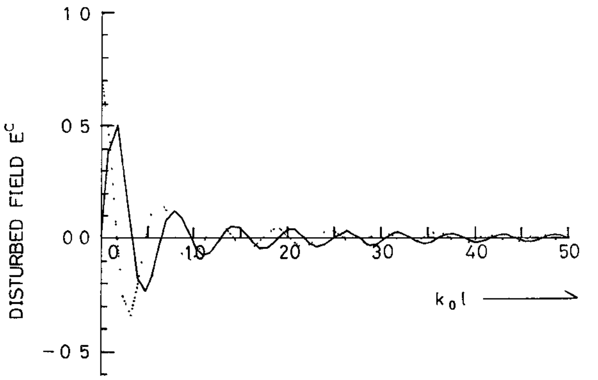

Fig. 4. Numerical examples of the disturbed field $E^C(\vec{x})$ along the upper side of waveguide 3 for the case of incidence from waveguide 1. The solid curve shows the real part and the dotted curve the imaginary part. The abscissa $k_0 l$ is the normalized distance from the junction point O' in Fig. 1.

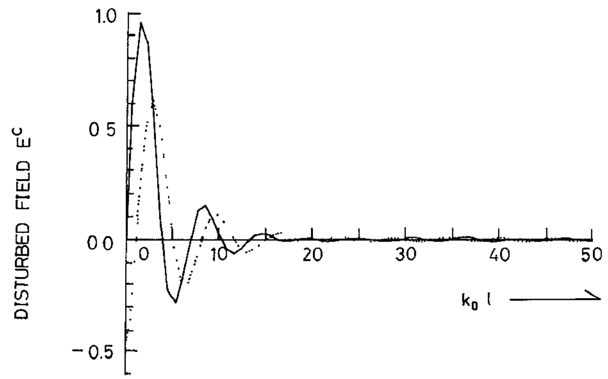

Fig. 5. Numerical examples of the disturbed field $E^C(\vec{x})$ along the upper side of waveguide 3 for the case of incidence from waveguide 2. The solid curve shows the real part and the dotted curve the imaginary part. The abscissa $k_0 l$ is the normalized distance from the junction point O' in Fig. 1.

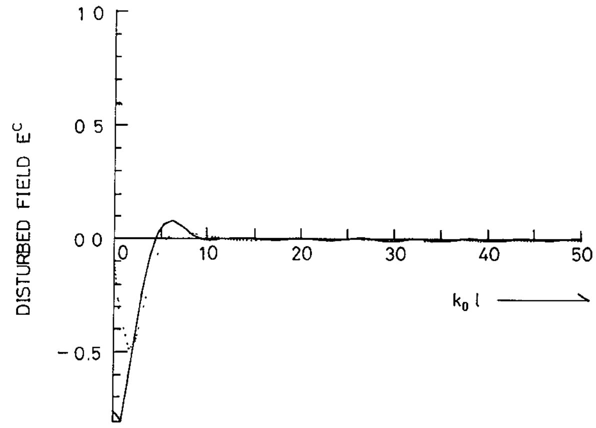

Fig. 6. Numerical examples of the disturbed field $E^C(\vec{x})$ along the upper side of waveguide 3 for the case of incidence from waveguide 3. The solid curve shows the real part and the dotted curve the imaginary part. The abscissa $k_0 l$ is the normalized distance from the junction point O' in Fig. 1.

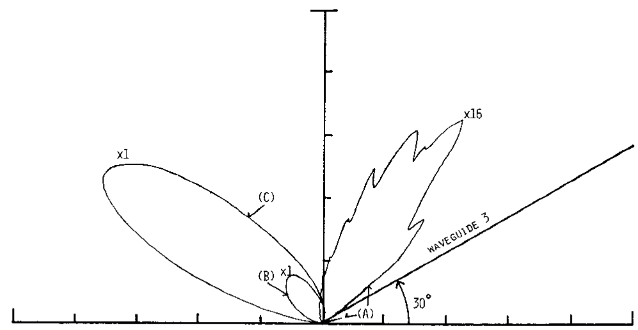

Fig. 7. Scattering patterns (A) for the case of incidence from waveguide 1, (B) for the case of incidence from waveguide 2, and (C) for the case of incidence from waveguide 3. Notice that (A) is magnified 16 times.

junction. The scattering patterns of each case are illustrated in Fig. 7. Note that the scattering pattern for the case of incidence from waveguide 1 is magnified 16 times. Since we could find no theoretical and experimental results in the literature to compare with these scattering patterns, we cannot discuss the accuracy of the results. However, the shapes of the scattering patterns are expected from a physical viewpoint.

Table I shows the numerical values of Γ_{ij}, Γ_{iS} and Γ_{TOTAL}. The results in parentheses are those obtained by the Born approximation. It is seen that the basic behavior of the wave propagation in the branching waveguide can be found by the Born approximation only qualitatively but not quantitatively. The validity of the Born approximation, however, depends on many parameters, such as the difference of the index of refraction between the surrounding space and the dielectric waveguides, the junction angle, and the width of waveguide 3.

We notice that the results by the moment method satisfy the energy conservation law well, but they satisfy reciprocity only approximately. We feel that this is due to the size of the triangles. Obtaining more accurate results requires division of waveguide 3 into a larger number of triangles.

TABLE I
Numerical Values of Reflected, Transmitted, Scattered, and Total Powers Normalized to the Incident Wave

Γ_{ij}	1	2	3	Γ_{iS}	Γ_{TOTAL}
1	0.0007 (0.0029)	0.6827 (0.7140)	0.2746 (0.1861)	0.0368 (0.0623)	0.9967 (0.9712)
2	0.7069 (1.2160)	0.0119 (0.0005)	0.0107 (0.0008)	0.2634 (0.1293)	0.9930 (1.3467)
3	0.2836 (0.5459)	0.0089 (0.0006)	0.0026 (0.0010)	0.7049 (0.5283)	1.0000 (1.0758)

Results in parentheses are those obtained by the Born approximation. Column i (1,2,3) shows the normalized transmitted power for the case of incidence from the ith waveguide and row j (1,2,3) shows the result in the jth waveguide.

XI. Conclusions

New forms of volume integral equations for wave propagation in dielectric branching waveguide based on an exact theory have been presented. The new integral equations have been solved approximately by the Born approximation and numerically by the moment method. The solutions are discussed from the viewpoint of energy conservation and reciprocity. The validity of the new volume integral equations has been demonstrated. Additional numerical results will be presented in a future paper.

The method using new volume integral equations is promising, since it can be extended to problems of a more general nature, i.e., the incident TM mode, and more complex configurations of branching waveguides. The basic idea is also applicable to techniques using boundary (surface) integral equations [20], [21] which are applicable to three-dimensional problems. This problem is currently under consideration.

Acknowledgment

The authors would like to acknowledge J. Fujimura, S. Rokuhara, and H. Yokomichi for their help in the numerical calculations.

References

[1] M. D. Feit and J. A. Fleck, Jr., "Light propagation in graded-index optical fibers," *Appl. Opt.*, vol. 17, pp. 3990–3998, Dec. 1978.

[2] J. van. Roey, J. van der Donk, and P. E. Lagasse, "Beam propagation method: Analysis and assessment," *J. Opt. Soc. Amer.*, vol. 71, pp. 803–810, July 1981.

[3] R. Baets and P. E. Lagasse, "Calculation of radiation loss in integrated-optic tapers and Y-junctions," *Appl. Opt.*, vol. 21, pp. 1972–1978, June 1982.

[4] O. Hanaizumi, M. Miyagi, and S. Kawakami, "Wide Y-junctions with low losses in three-dimensional dielectric optical waveguides," *IEEE J. Quantum Electron.*, vol. QE-21, pp. 168–173, Feb. 1985.

[5] K. Ogusu, "Transmission characteristics of single-mode asymmetric dielectric waveguide Y-junctions," *Opt. Commun.*, vol. 53, pp. 169–172, Mar. 1985.

[6] K. Ono and S. Sawa, "Propagation characteristics of a multimode Y-junction waveguide in lens-like media," *Trans. IECE Jpn.*, vol. J68-C, pp. 869–870, Oct. 1985.

[7] M. Seino, H. Nakajima, Y. Daito, I. Sawaki, and K. Asama, "Optical waveguide analysis using the Fourier transform and its application to intersecting waveguide," *Trans. IECE Jpn.*, vol. J66-C, pp. 732–739, Oct. 1983.

[8] D. Marcuse, "Radiation losses of tapered dielectric slab waveguides," *Bell Syst. Tech. J.*, vol. 49, pp. 273–290, Feb. 1970.

[9] I. Anderson, "Transmission performance of Y junctions in planar dielectric waveguide," *IEE J. Microwaves, Optics and Acoust.*, vol. 2, pp. 7–12, Jan. 1978.

[10] H. Sasaki and I. Anderson, "Theoretical and experimental studies on active Y-junction in optical waveguide," *IEEE J. Quantum Electron.*, vol. QE-14, pp. 883–892, Nov. 1978.

[11] H. Yajima, "Dielectric thin film optical branching waveguide," *Appl. Phys. Lett.*, vol. 22, pp. 647–649, June 1973.

[12] W. K. Burns and A. F. Milton, "Mode conversion in planar-dielectric separating waveguides," *IEEE J. Quantum Electron.*, vol. QE-11, pp. 32–39, Jan. 1975.

[13] M. Kuznetsov and H. A. Haus, "Radiation loss in dielectric waveguide structures by the volume current method," *IEEE J. Quantum Electron.*, vol. QE-19, pp. 1505–1514, Oct. 1983.

[14] M. Kuznetsov, "Radiation loss in dielectric waveguide Y-branch structure," *J. Lightwave Technol.*, vol. LT-3, pp. 674–677, June 1985.

[15] A. W. Snyder, "Radiation losses due to variations of radius of dielectric or optical fibers," *IEEE Trans. Microwave Theory Tech.*, vol. MTT-18, pp. 608–615, Sept. 1970.

[16] K. Tanaka and M. Kojima, "Analysis of dielectric branching waveguide by integral equations," *Tech. Rep. IECE Jpn. EMT-86-108*, Oct. 1986.

[17] J. H. Richmond, "Scattering by a dielectric cylinder of arbitrary cross section shape," *IEEE Trans. Antennas Propagat.*, vol. AP-13, pp. 334–341, May 1965.

[18] J. H. Richmond, "Scattering by thin dielectric strips," *IEEE Trans. Antennas Propagat.*, vol. AP-33, pp. 64–68, Jan. 1985.

[19] R. E. Collin, *Field Theory of Guided Waves*. New York: McGraw-Hill, 1960, p. 485.

[20] N. Morita, "Surface integral representations for electromagnetic scattering from dielectric cylinders," *IEEE Trans. Antennas Propagat.*, vol. AP-26, pp. 261–266, Mar. 1978.

[21] T. K. Wu and L. L. Tsuai, "Numerical analysis of electromagnetic fields in biological tissues," *Proc. IEEE*, vol. 62, pp. 1167–1168, Aug. 1974.

Kazuo Tanaka (M'75) was born in Mie Prefecture, Japan, on June 7, 1947. He received the B.E., M.E., and Ph.D., degrees in electrical communication engineering from Osaka University, Osaka, Japan, in 1970, 1972, and 1975, respectively.

In 1975, he became a Research Associate in the Department of Electrical Engineering at Gifu University and Associate Professor in the Department of Electronics and Computer Engineering there in 1985. His research work since 1970 has been on relativistic electromagnetic theory, computational electromagnetics, and radiographic image processing and he is currently interested in the CAD of integrated optical circuits.

Dr. Tanaka is a member of the Institute of Electronics, Information and Communication Engineers of Japan and the Information Processing Society of Japan.

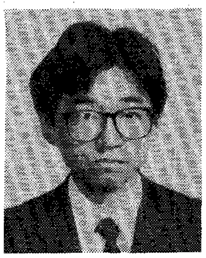

Masaaki Kojima was born in Nagoya, Japan, on April 28, 1963. He received the B.S. and M.S. degrees in electrical engineering from Gifu University, Gifu, Japan, in 1986 and 1988, respectively.

Since 1988 he has been employed by the Nippon Telegraph and Telephone Corporation (NTT), Tokyo, Japan.

Mr. Kojima is a member of the Institute of Electronics and Communication Engineers of Japan.